

DRAFT

Report #05-032

Probabilistic Representation of the Threat and Consequences of Weapon Attacks on Commercial Aircraft

Caffrey, J. & Masri, S.

CREATE REPORT
Under FEMA Grant EMW-2004-GR-0112

November 29, 2005



**Center for Risk and Economic Analysis of Terrorism Events
University of Southern California
Los Angeles, California**

This research was supported by the United States Department of Homeland Security through the Center for Risk and Economic Analysis of Terrorism Events (CREATE) under grant number N00014-05-0630. However, any opinions, findings, and conclusions or recommendations in this document are those of the authors and do not necessarily reflect views of the United States Department of Homeland Security.

Probabilistic Representation of the Threat and Consequences of Weapon Attacks on Commercial Aircraft

CREATE Report

29 November 2005

John P Caffrey, Research Assistant Professor
Sami F Masri, Professor

Department of Civil and Environmental Engineering
University of Southern California

Acknowledgment

This research was supported by the United States Department of Homeland Security through the Center for Risk and Economic Analysis of Terrorism Events (CREATE), grant number EMW-2004-GR-0112. However, any opinions, findings, and conclusions or recommendations in this document are those of the authors and do not necessarily reflect views of the U.S. Department of Homeland Security.

Table of Contents

EXECUTIVE SUMMARY 4

INTRODUCTION 5

APPROACH 7

DEVELOPMENT OF CIVILIAN AIRCRAFT PROJECTED AREA MODEL 9

INTERPOLATION OF THE PROJECTED AREA 18

DEVELOPMENT OF THE AIRCRAFT FLIGHT PATH 20

WEAPON LETHALITY MODEL 26

METHODOLOGY FOR LOCATING AIRCRAFT DEBRIS SCATTER 27

POTENTIAL RESEARCH 36

CONCLUSIONS 38

REFERENCES 39

Appendix 1-GIS INTERFACE DESIGN DOCUMENT 40

EXECUTIVE SUMMARY

The Department of Homeland Security has determined that external weapon threats due to surface-air missiles, as well as some conventional weapons, pose a serious threat to commercial aircraft. Many factors that are highly random in nature (such as the type of missile or weapon used, the proximity and orientation of the warhead/weapon detonation with respect to the aircraft, the structural characteristics of the aircraft, and the fragility level of the damaged aircraft components, such as fuel tank, engine, flight control, etc) influence the level of hazard to which a target aircraft is subjected, as well as the subsequent damage of an exploding aircraft debris on the ground below.

In view of the numerous uncertain decision and performance variables encountered in the modeling of scenarios involved in the assessment of the consequences of MANPADS attacks on civilian aircraft, there is a need for the development of a general probabilistic methodology for multi-aircraft/multi-weapon attacks. Even though a considerable amount of research has been previously done, on related topics, by government agencies and research labs, virtually nothing of quantitative nature is available in the open literature concerning this topic.

This report presents an initial stage of a general methodology for developing and implementing a modular software package that incorporates a variety of computational modules for quantifying and propagating the uncertainties associated with the specification of a postulated terrorist attack. Among the main random parameters considered are: the aircraft location and orientation, the aircraft flight path trajectory, the aircraft characteristics, the probability of a weapons-induced crash, and the random distribution of explosion debris, etc. The ultimate aim is to provide a quantitative (probabilistic) measures of the consequences of typical MANPADS attacks on typical civilian aircraft.

While an arbitrary scenario was used to demonstrate the implementation of all phases of the chain of events encompassing the randomness imbedded in the numerous input parameters to the computational engine, the systems-based architecture is extremely flexible, and would easily allow the user to replace specific modules with updated ones that reflect needed levels of analysis sophistication, weapons performance data, structural failure analysis, aircraft equipment vulnerability data, more accurate physics-based modeling of debris dispersal, etc.

In order to maximize the utility of the simulation package, its modules are designed to easily interface with a GIS-based package in which other related threat and consequence scenarios can be conveniently specified, and their outcomes evaluated and displayed in near real time, to assist decision makers in quickly investigating a broad range of postulated attack scenarios.

INTRODUCTION

Background:

The Department of Homeland Security has determined that external weapon threats due to surface-air missiles, as well as some conventional weapons, pose a serious threat to commercial aircraft. Many factors that are highly random in nature (such as the type of missile or weapon used, the proximity and orientation of the warhead/weapon detonation with respect to the aircraft, the structural characteristics of the aircraft, and the fragility level of the damaged aircraft components, such as fuel tank, engine, flight control, etc) influence the level of hazard to which a target aircraft is subjected, as well as the subsequent damage of an exploding aircraft debris on the ground below.

Literature Review:

A considerable amount of research and development effort has been devoted in the past few decades to the discipline of aircraft combat survivability (Ball, 2003). An excellent reference on this subject is the 2003 AIAA publication titled "The Fundamentals of Aircraft Combat Survivability Analysis and Design." The focus of this well-known book is on the capability of an aircraft to withstand or avoid a man-made hostile environment. And while some of the general issues discussed in the cited reference in the context of military aircraft are applicable to civilian aircraft exposed to MANPADS engagements, the material is of limited use for the probabilistic assessment of the risk and consequences of MANPADS attacks on civil aircraft.

After an extensive effort to gather all available information in the public domain concerning the goals of this project, it became clear that the research topic under consideration has been, and continues to be, of considerable importance and interest to government authorities. A significant level of effort by numerous groups (primarily in military branches) over a long period of time has been devoted to assessing the vulnerability of aircraft to MANPADS attacks. However, most of the relevant technical and quantitative information needed to implement the goals of the study under discussion are not available in the public domain.

The authors contacted Donald L Wesenberg, at Sandia National Lab (Wesenberg, 2004), who has, for a long period of time, been conducting state-of-the-art research and investigations of terrorist attacks on aircraft. However, his efforts have focused on the sophisticated analysis of the interaction between aircraft and structures (crash phenomena). He has been developing high-fidelity computational models of large civilian aircraft that crash into civil structures. These models are designed to provide an accurate simulation of the multi-physics phenomena involved in the complete aircraft-structure-fuel- propulsion-control system, and to subsequently reproduce all the physics involved in the crash of fuel-laden aircraft and the attendant thermodynamic effects involving the burning fuel. These studies did not focus on the interaction between the aircraft and weapon.

Furthermore, in order to avoid as much as possible “re-inventing the wheel” in regard to reproducing investigations of MANPADS on civilian aircraft, the authors and colleagues devoted an extensive effort to contacting and meeting experts in the field of aircraft survivability under hostile actions at the China Lake facility of the Navy (NAVAIR Weapons Division, and the Titan Corporation) who are involved in the modeling and simulation of aircraft involved in terrorist activities. It was found that indeed a number of comprehensive studies and tests have been performed at several military locations to assess the performance of MANPADS and other weapons on aircraft, but none of the resulting quantitative information about the performance of the weapons or the damage sustained by target aircraft, is available in the open literature.

Scope:

Due to the unavailability in the open literature of computational models of representative aircraft that can be used in simulation studies of MANPADS-related studies to assess the survivability of target aircraft, and in view of the limited resources available to perform the task under discussion, it was decided that the initial phase of the study would focus on the following subtasks:

- Development of a simplified, but quite detailed, finite element model of a generic aircraft.
- Using the projected aircraft surface ("target cross-section") as a surrogate for the degree of vulnerability of the aircraft to a MANPADS attack.
- Development of a general probabilistic framework for conducting a broad class of uncertainty studies based on Monte Carlo simulation techniques to assess the probability of a single or multiple-set of aircraft to be attacked by a single or multiple-set of weapons.
- Planning of a Geographic Information System (GIS) interface to exhibit the “Vulnerability Surface” overlaying an arbitrary geographic region surrounding a specific airport.
- Developing physics-based approaches for assessing the consequences of a successful shooting down of an aircraft by tracking the resulting debris distribution at ground level.

Goal:

The main goal of this study was to develop and apply computational tools, based on probabilistic structural dynamics approaches, to represent the threat as well as the consequences of external weapon threats to aircraft, so that the resulting format can be utilized in an assessment of the economic effects of such threats.

APPROACH

Development of General Probabilistic Methodology for MANPADS Weapon Attacks on Civil Aircraft

One of the primary goals of this project was to develop a GIS based tool to help authorities with the response planning to help mitigate the disaster that would result from a terrorist attack on a civil aircraft. If a terrorist attack does happen, it is likely to occur in a large metropolitan area with the primary airport located within the heart of the region. The Los Angeles basin is just such a region with LAX providing the majority of commercial airline traffic. If a terrorist group is planning a MANPADS attack against civil aircraft, the Los Angeles area would be high on their list. Planning for such an attack would be prudent and having a tool for researchers and disaster relief planners would be desirable. This goal dictated the approach taken in developing the computer program. The user should not have to enter any commonly available information such as airline flight data or airport landing approach and departure procedures. At same time, the computer program must be modular in design such that if the researcher using the tool does not like the assumptions made, such as debris velocity after a MANPADS explosion, he may simply replace the subroutine with one that is more to his liking. Also, all of the examples throughout this report are based on flights into and out of LAX, the approach taken allows the airport to be changed with the use of appropriate input files. With this mind, this section will describe the approach used in the GIS based threat analysis tool. An overview of the methodology is shown in Figure 2.

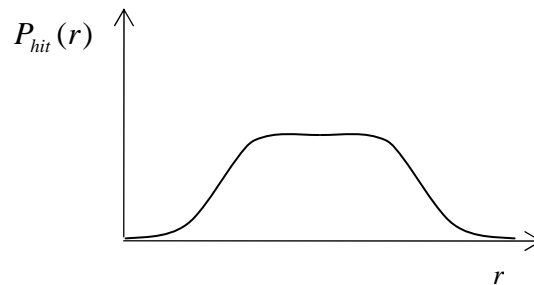
The methodology for MANPADS Attacks on Civil Aircraft assume that the following input parameters are specified:

1. The location and geometric configuration of a specific airport such as Los Angeles International Airport (LAX)
2. A specific date and time (for which commercial flight schedules of arrivals and departures are available from the airlines using LAX).
3. The location of the MANPADS launch site, or general vicinity of the launch area
4. The type of MANPADS weapon to be used

After the appropriate input parameters are selected by the user through the GIS interface, the computer program:

1. determines the trajectory of incoming and outgoing aircraft in the region, and estimates the location (in 3D space) of each such aircraft within a radius R_0 from LAX (e.g., $R_0 = 15$ miles). Let the selected aircraft be designated as L_1, L_2, \dots, L_n .
2. assumes that the exposure/susceptibility analysis will be done using a ground-launching area whose "coarseness" is A_0 (e.g., $A_0 = 1$ square mile).

3. generates a pseudo-random number, randomly selects a specific location characterized by spatial coordinates $\{dx, dy\}_i$ in a 2D plane to determine the location of all of the aircraft. Then, for each such point, determine the radial distance r_i to each target aircraft L_i , and computes the normalized, projected area A_j of airplane L_j in the direction of a projectile launched from location i . The quantity A_j is computed by determining the reference airplane projected area and then normalizing the result by the maximum projected area. Hence, the numerical range of A_j is between 0.0 – 1.0.
4. to account for the variation in the “lethality” of the attack weapon with the distance between launch position and aircraft location, assume that a deterministic curve is available that provides the functional dependence of the probability of hit $P_{hit}(r)$ as a function of the separation distance r . For example, such a curve may have small values at too close a distance, reaches its maximum value of P_0 within a specified region, and then falls asymptotically to zero for very far distances as shown in Figure 1.



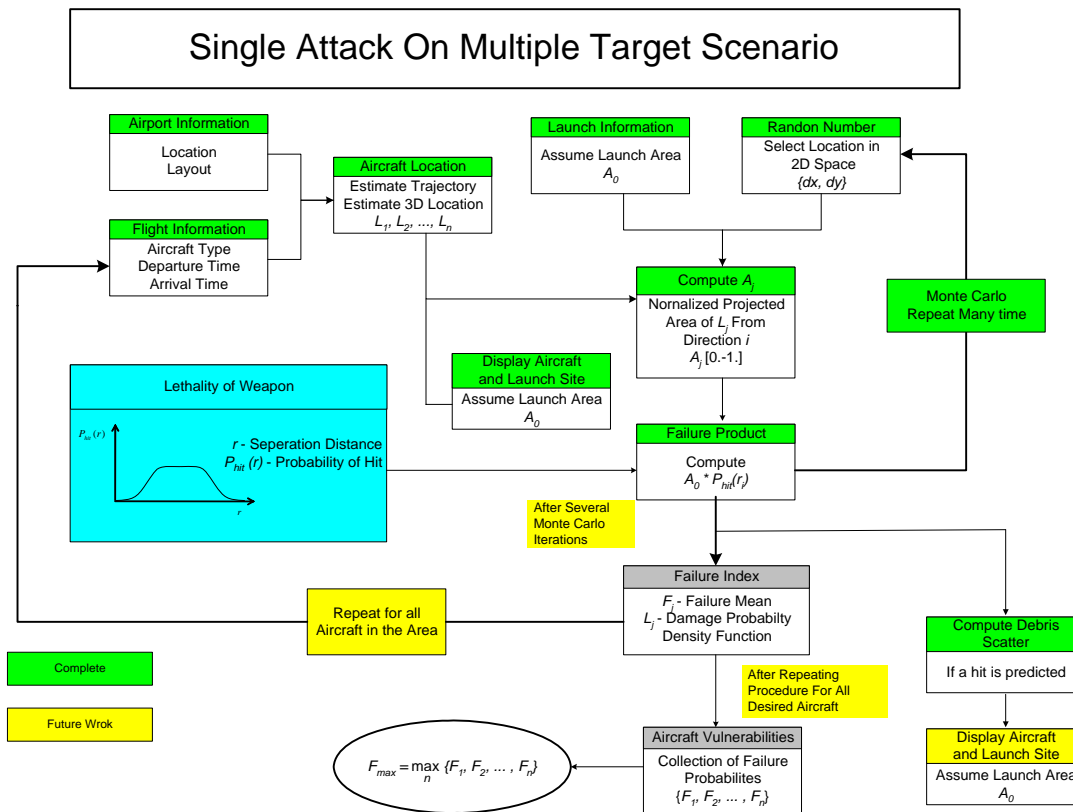
Functional dependence of weapon effectiveness on weapon-target distance.

Figure 1

5. randomizes the location of the launch site within the discrete analysis area in the area selected by the user through the GIS interface. Then for each iteration (randomized location), compute the product $A_j P_{hit}(r_i)$. By repeating this operation a very large number of times using conventional Monte Carlo simulation methods, one can obtain the distribution of simulated encounters (i.e., obtain the mean F_j of failure and its corresponding probability density function of the aircraft L_j damage index).
6. repeats the above procedure for each aircraft in the landing path, as well as the take-off path, the expected failure probabilities for the collection of vulnerable aircrafts can be obtained as $\{F_1, F_2, \dots, F_n\}$.
7. assumes a single attack (weapon launch), then the worst case scenario would correspond to the largest probability among the set of n probabilities computed above:

$$F_{\max} = \max_n \{F_1, F_2, \dots, F_n\}$$

8. computes at the users request, the debris scatter of an aircraft assuming it has been hit by a MANPADS launch followed by an explosion. The user selects the aircraft of interest and the number of particles (aircraft debris). The computer program automatically debris fallout pattern and debris area on the ground. The results are plotted in the GIS Map

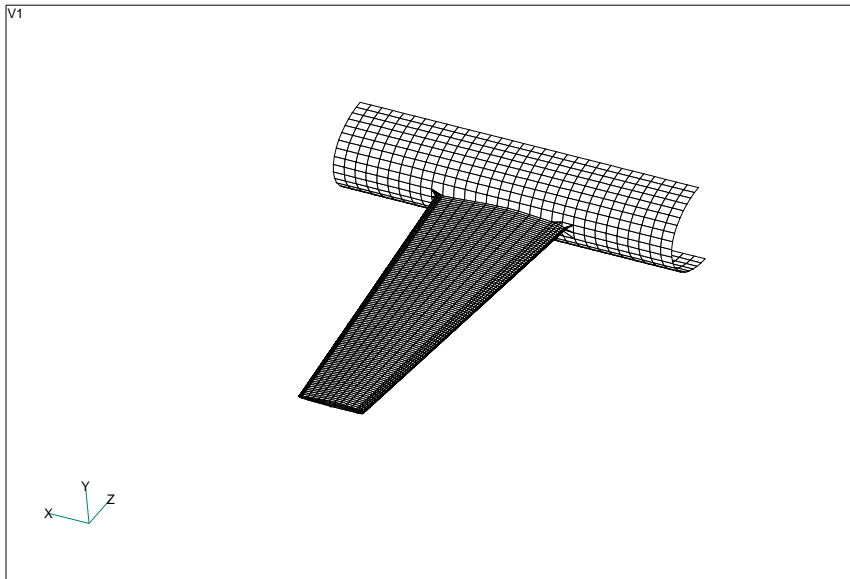


Single Attack on Multiple Targets Scenarios
Figure 2

DEVELOPMENT OF CIVILIAN AIRCRAFT PROJECTED AREA MODEL

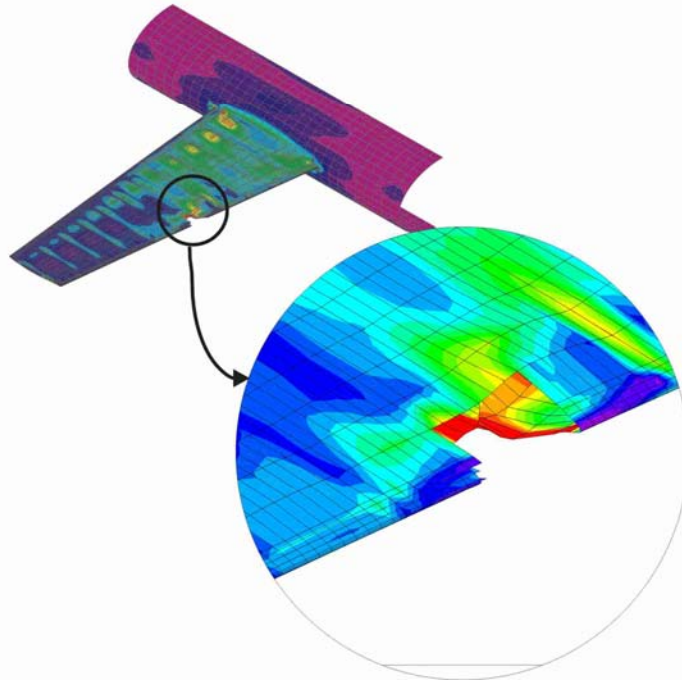
The development of aircraft computational models suitable for structural analysis can be very time consuming, as it is necessary to know the main structural members in the aircraft. Ideally, the aircraft manufacturers would supply such a model, which at this point looks unlikely. The second best scenario would be to obtain the design information from the aircraft manufactures to generate a computer model, which seems unlikely at this point. The last option is to construct the computational model from scratch based on published cross-sectional views. Again, this is very time consuming. The resulting finite

element model (FEM) can be used to assess the probability of aircraft failure as well as an estimate of the debris size, should a missile attack be successful. As an example, consider a simplified model of an aircraft wing structure as shown in Figure 3.



Simple Finite Element Model of an Aircraft Wing
Figure 3

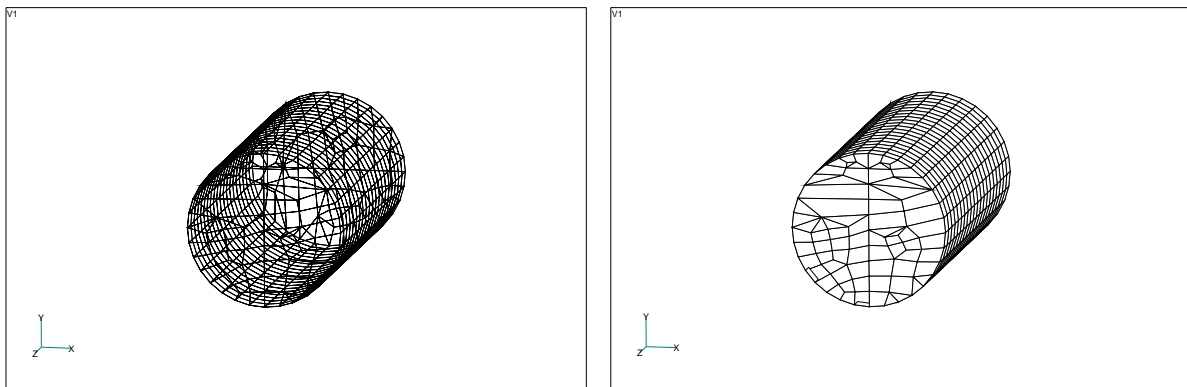
The missile is assumed to graze the leading edge of the aircraft and damage the wing structure as shown in Figure 4. A finite element analysis is performed to find the stress in area of the impact. The damage is modeled by removing elements in the damage region. Based on the computed stress, the likelihood of failure and type of failure will be determined. Due to the statistical nature of the approach, several analyses will need to be performed for a given scenario. The wing structure shown is to demonstrate the approach used, a more realistic structural model, which contains the critical structural elements, can be developed to include as much detail as necessary for the level of sophistication desired.



Wing Finite Element Model Results
Figure 4

2. Computation of Aircraft Projected Area Relative to Weapon Trajectory

The procedure used to compute the projected area of an aircraft structure is similar to the Z-buffer technique used for hidden line display. This approach is best described with the use of an example. Consider the simple cylinder model shown in Figure 5.



Cylindrical Test Structure
Figure 5

The model shown in Figure 5 is a surface FEA model, which was created from scratch (not imported) to demonstrate the concept; an actual aircraft model will be presented later in this section. The procedure to obtain the cross-sectional area as seen by an incoming missile is as follows:

1. Determine the location, direction, and orientation of the aircraft and the location of the MANPADS launch using the GIS graphical interface. This position and orientation information will eventually be computed and passed as parameters from the GIS system. Using this information, the vector direction from the MANPADS launch site to the aircraft and the rigid body relationship between the two are computed from which the rigid body transformations can be determined in matrix form. The matrix transformation matrices are used to rotate the finite element model to the X-Y viewing plane, that is, the plane normal to the line of sight of the missile. It is interesting to note that the orientation of the aircraft is specified in spherical coordinates relative to the aircraft's own reference system corresponding the pitch, roll, and yaw of the aircraft, terms which are familiar to aviation personnel. The location and heading of the aircraft is specified in rectilinear coordinates. The transformation matrices are as follows:

$$\{X\}_v = [\phi]_{rv}^T [\phi]_{\phi r}^T \{X\}_l$$

Where:

$\{X\}_l$ = Location of the facet vertices in local coordinates

$\{X\}_v$ = Location of the facet vertices in view coordinates

$[\phi]_{rv}^T$ = Transformation from rectangular space coordinates to view coordinate space

$[\phi]_{\phi r}^T$ = Transformation from aircraft local spherical system to rectangular system

The FORTRAN implementation of the matrix $[\phi]_{rv}^T$ transformation subroutine is as follows:

```
subroutine transform1(idir,theta)
include 'commons.txt'
character*100 fileout1
character*80 aline
dimension c(3,3)
pi=atan(1.)*4.
! Convert angles to radians
thetal=theta*pi/180.
The directions 1,2,3 correspond to dir x,y,z in global space
if(idir .eq. 1) then
  c(1,1) = 1.
  c(1,2) = 0.
  c(1,3) = 0.
  c(2,1) = 0.
  c(2,2) = cos(thetal)
  c(2,3) = -sin(thetal)
```

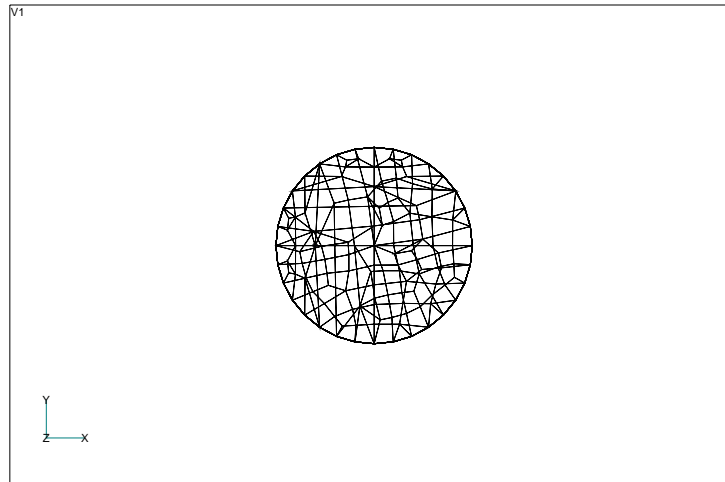
```

      c(3,1) = 0.
      c(3,2) = sin(thetal)
      c(3,3) = cos(thetal)
    else if(idir .eq. 2) then
      c(1,1) = cos(thetal)
      c(1,2) = 0.
      c(1,3) = sin(thetal)
      c(2,1) = 0.
      c(2,2) = 1.
      c(2,3) = 0.
      c(3,1) = -sin(thetal)
      c(3,2) = 0.
      c(3,3) = cos(thetal)
    else if(idir .eq. 3) then
      c(1,1) = cos(thetal)
      c(1,2) = -sin(thetal)
      c(1,3) = 0.
      c(2,1) = sin(thetal)
      c(2,2) = cos(thetal)
      c(2,3) = 0.
      c(3,1) = 0.
      c(3,2) = 0.
      c(3,3) = 1.
    else
      print*, 'Bad idir argument to transform1'
      pause
      stop
    endif
  ! the matrix transformation is complete
  ! perform the actual rotate
  do i=1,numnode
    xnew = c(1,1)*rnodeloc(i,1) + c(1,2)*rnodeloc(i,2) + C(1,3)*rnodeloc(i,3)
    ynew = c(2,1)*rnodeloc(i,1) + c(2,2)*rnodeloc(i,2) + C(2,3)*rnodeloc(i,3)
    znew = c(3,1)*rnodeloc(i,1) + c(3,2)*rnodeloc(i,2) + C(3,3)*rnodeloc(i,3)
    rnodeloc(i,1) = xnew
    rnodeloc(i,2) = ynew
    rnodeloc(i,3) = znew
  enddo
  return
end

```

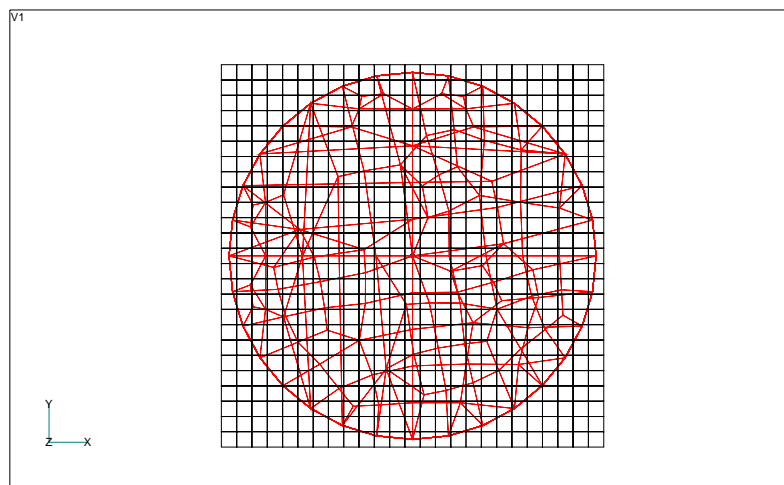
The FORTRAN implementation of the transformation matrix $[\phi]_{\phi}^T$ is similar that shown for $[\phi]_{rv}^T$ and has not been included here.

2. Within the X-Y viewing plane, determine the extent of the finite element model nodes. This is accomplished by finding the extreme x and y coordinates of the transformed model in the viewing coordinates. For this example assume that the viewing axis is along the axis of the cylinder as shown in Figure 6.



Cylinder in the Viewing Coordinates
Figure 6

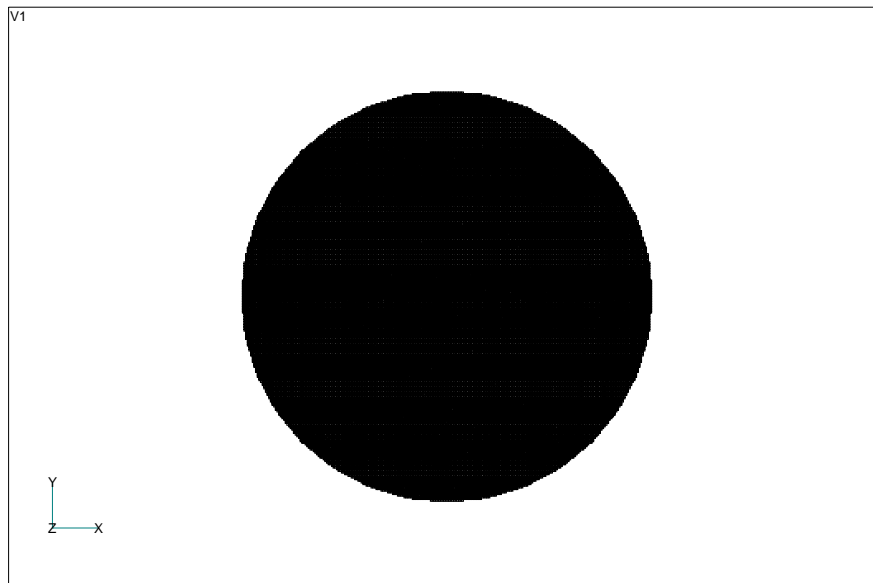
3. Next overlay a fine mesh over the mesh as shown of Figure 6. The mesh shown in the figure is intentionally made coarse (25 by 25) so that the underlying FEA mesh can be seen in Figure 7. The coarser the grid, the more jagged the outline of the projected area but the resulting estimate of the projected area can still be reasonably accurate.



Overlay mesh
Figure 7

4. Once the mesh is obtained, each element in the FEA model is reviewed to determine which of the subdivision centroids in the mesh lie within the projected area of the element. If the centroid does lie within the projected area, then the subdivision is flagged as being part of the overall projected area. Otherwise, it is not flagged as being part of the overall projected area, and is not included in the area projection calculation. After all of the elements are reviewed, then the sum of all the flagged subdivision areas is computed to get the total projected area as

shown in Figure 8. In this example, the simple cylinder had a diameter of 10 inches and length of 20 inches. The projected area from the computer program is calculated as 78.1 and the theoretical area is 78.6 in²

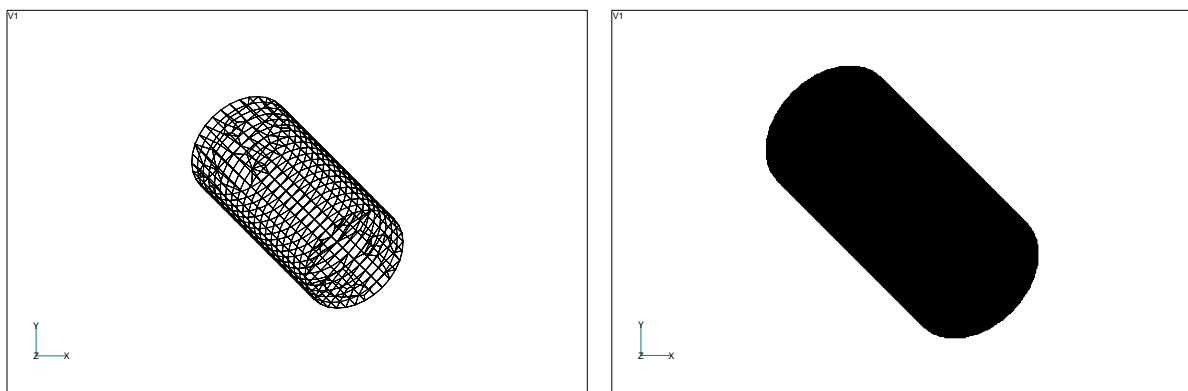


Projected Area of the Cylinder

Figure 8

As mentioned, the subdivisions shown in Figure 6 are rather coarse. For the actual runs, a much finer grid is used, thereby increasing the accuracy of the projected area. A mesh size of 250 by 250 appears to give excellent results, and is still relatively quick to process. To improve the speed, the program performs some internal screening to minimize the number of element interior checks needed.

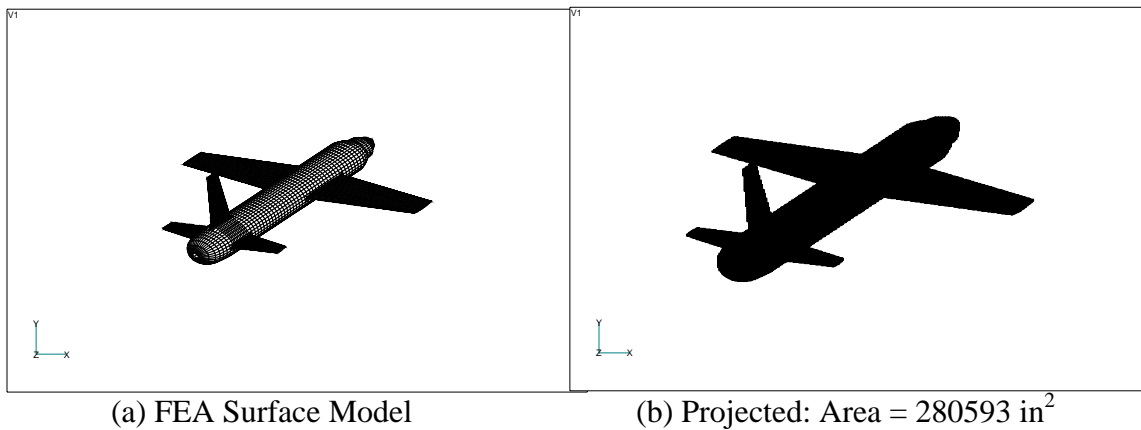
As another example, consider the cylinder rotated so that the viewing axis is not along one of the principal directions as shown in Figure 9. As can be seen, the projected area shown is an accurate representation of the skewed cylinder.



Skewed Cylinder Example

Figure 9

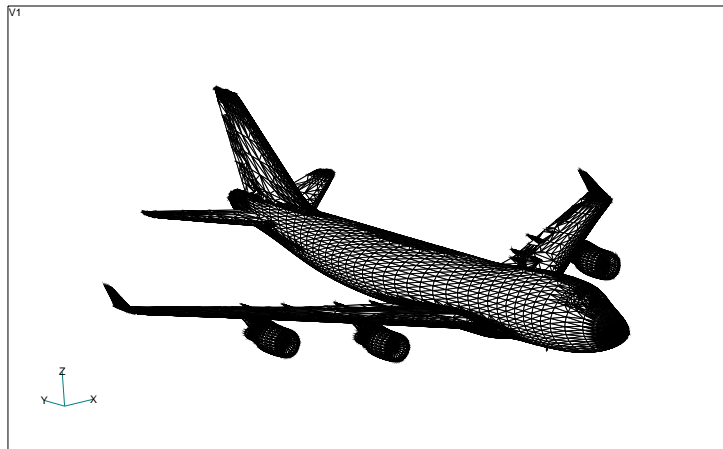
To test the speed and stability of the algorithm used, a sample FEA model of a generic aircraft was constructed to validate the program. The sample FEA aircraft model consists of 29,476 nodes and 29,155 elements and is shown in Figure 10. The aircraft model is a surface model only, that is, there is no interior structure. Also, the model was not meant to be of any particular aircraft; rather, it is a generic in nature. It is interesting to note the total surface area of the aircraft is 1,083,385 in². The algorithm is very stable and relatively fast, completing the projected area computation in about 4 minutes. This speed will not be fast enough when the program is imbedded in the GIS system, where the user expects the results interactively. Therefore, another program was developed to use interpolation values obtained from pre-computed projected areas of the model when speed of execution speed is desired. It is envisioned that a database of commercial aircraft surface models of various resolution would be created and be queried by the GIS system or the spawned processes, as needed. It would be unreasonable to perform mesh consolidation on the fly. The projected area of the generic aircraft is shown in Figure 10.



Aircraft FEA Generic Model to Test Project Algorithm
Figure 10



(a) Rendered Model



(b) Faceted Representation



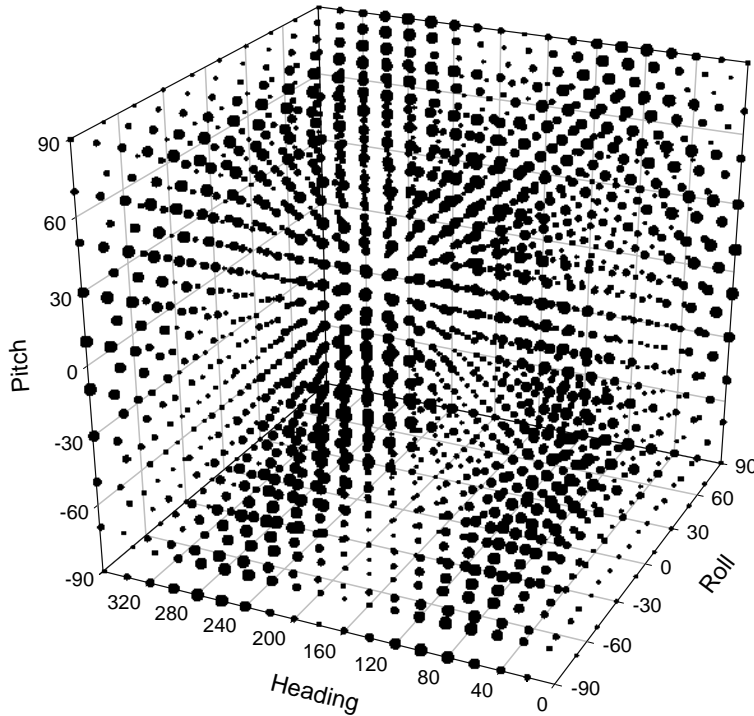
(c) Projected Area

Boeing 747 Area Projected Example
Figure 11

The last example is most realistic in that it is an accurate model of a Boeing 747 as shown in Figure 11. To perform the projected area calculations on the aircraft, a very detailed surface model was obtained commercially. The rendered model of the Boeing 747 is shown in Figure 11a. This surface model representation was converted to a faceted model in STL format as shown in the Figure 11a. The custom software written to compute area projections has the option of reading a stereo lithographic (STL) file and converting it to the appropriate FEA surface model. Using this STL import capability, the area projection program is able to read the Boeing 747 surface geometry and compute the projection map as shown. The same procedure can be applied to any number of aircraft models, with various resolutions, with relative ease.

INTERPOLATION OF THE PROJECTED AREA

Computation of the project area is computationally intense which can take several minutes to compute on an average desktop PC. The goal was to develop an interactive GIS tool so that it can be used to perform what-if scenarios and multi-aircraft, multi-threat studies. To accomplish this, performing a projected area calculation on the fly is not practical, as the user would be frustrated waiting too long for the results, especially when many aircraft are considered. By pre-computing and storing the projected area of an aircraft for a range of all pitch, roll, and heading angles of interest, one can simply use an interpolation function to estimate the projected area of the aircraft for any desired value of orientation angles. To demonstrate this concept, the projected area of the Boeing 747 was computed for a range of roll of -90 to 90 degrees, pitch of -90 to 90 degrees, and a heading of 0 to 360 degrees at 10-degree intervals. This resulted in a database with 13357 entries. Figure 12 shows a plot of all of the computed points in 3-D space where the area of each plotted point is proportional to the value of the projected area. It is not expected that the reader can determine a projected area using the three-reference angle from the plot shown in Figure 12, however, it does provide some insight into the procedure. It can be seen that there is no large discontinuities in the size of the dots indicating the interval values of 10 degrees is adequate. It also demonstrates the completeness for the database showing no holes exist in the solution space.



3-D plot of the Projected Areas for the Sample Aircraft
Figure 12

The procedure for interpolating the values of the database for a given set of reference angles is as follows:

For a given set of reference angles, ϕ , θ and ψ representing the roll, pitch, and heading of the aircraft, the database is searched to find the vertices of the bounding cube. For example, suppose, $\phi = 20^\circ$, $\theta = -30^\circ$ and $\psi = 50^\circ$ the database is searched to locations shown in table 1.

Vertex	Roll	Pitch	Heading	Projected Area
1	-70	20	-50	1019.212
2	-70	20	-30	1084.010
3	-70	40	-50	1117.591
4	-70	40	-30	1104.699
5	-50	20	-50	872.6975
6	-50	20	-30	915.3687
7	-50	40	-50	999.7555
8	-50	40	-30	975.6047

Example: Vertices of the bounding Cube
Table 1

The values shown in Table 1 are used to compute a 3-D linear planar surface using a least-squares curve fitting routine. The resulting equation of the surface for this example is:

$$\text{Area} = 509.88 - 7.0261 \cdot x + 3.8296 \cdot y + .88032 \cdot z$$

Substituting for x , y , and z

Yields $\text{Area} = 927.2375$

The time required to read the database file, locate the bounding vertices, and interpolate the results is a small fraction of second resulting in no perceivable lag.

DEVELOPMENT OF THE AIRCRAFT FLIGHT PATH

Most if not all of the daily commercial flight activity is available on the web and can be downloaded. The form of the database makes the flight information easily understood by the average user, however, it is not in a convenient form for rapid searching. A sample of the flight schedule showing the departure flights for LAX on a particular day in January 2005 is shown in Figure 14.

Flight	Frm	Departs	To	Arrives	Typ	Meal	Freq	Begins	Until	OperatedBy
AA 7370	LAX	8:30pm	AKL	6:00am	744	DR	MTWTFSS	01JAN05	17MAR05	QANTAS
BA 7302	LAX	8:30pm	AKL	6:00am	744	M	MTWTFSS	01JAN05	17MAR05	QANTAS
QF 26	LAX	8:30pm	AKL	6:00am	744	DR	MT.TFSS	01JAN05	17MAR05	
AA 7190	LAX	9:25pm	ANC	1:52am	737		M.WTFSS	01JAN05	03JAN05	ALASKA
AA 1182	LAX	9:00am	AUS	1:55pm	M80		MTWTF.S	01JAN05	09JAN05	
AA 1280	LAX	11:20am	AUS	4:17pm	M80		MTWTFSS	01JAN05	09JAN05	
AA 1716	LAX	6:00pm	AUS	10:49pm	M80		MTWTFSS	01JAN05	30JAN05	
AA 8257	LAX	0:40am	BJX	5:40am	320	M	MTWTFSS	01JAN05	11JAN05	MEXICANA
AA 1974	LAX	11:00am	BNA	4:57pm	M83	L	MTWTFSS	01JAN05	09JAN05	
AA 7302	LAX	11:55pm	BNE	7:55am	744	RMS	02JAN05	20MAR05	QANTAS
QF 176	LAX	11:55pm	BNE	7:55am	744	RMS	02JAN05	20MAR05	
AA 7558	LAX	9:20am	BOI	12:10pm	CR7		MTWT..S	02JAN05	06JAN05	HORIZON AIR_
AA 7560	LAX	8:35pm	BOI	11:30pm	CR7		MTWT..S	01JAN05	06JAN05	HORIZON AIR_
AA 148	LAX	4:10pm	BOS	0:28am	738	D	MTWTFSS	01JAN05	30JAN05	
QF 3009	LAX	4:10pm	BOS	0:28am	738	D	MTWTFSS	01JAN05	30JAN05	AMERICAN

Sample of Flights leaving LAX
Figure 13

To efficiently read and process the flights in the area, the flight information as shown in Figure 13 is reformatted into a new database to provide for rapid searching. A sample of the reformatted database is shown in Figure 14.

AA ,6939,SEA,LAX,ALASKA ,	2130,	2135,	1220,	1372,	T,	T,	T,	T,	F,	T,	1281,	1130
QF ,3102,JFK,LAX,AMERICAN,	2077,	2128,	1260,	1432,	T,	T,	T,	T,	F,	T,	1127,	1130
AA ,6772,SEA,LAX,ALASKA ,	1983,	2080,	1277,	1433,	T,	T,	T,	T,	T,	T,	1281,	1130
QF ,3758,SEA,LAX,ALASKA ,	1983,	2080,	1277,	1433,	T,	T,	T,	T,	T,	T,	1281,	1130
AA ,6798,PDX,LAX,ALASKA ,	2081,	2129,	1308,	1439,	T,	T,	T,	T,	T,	T,	1238,	1130
QF ,3718,PDX,LAX,ALASKA ,	2081,	2129,	1308,	1439,	T,	T,	T,	T,	T,	T,	1238,	1130
QF ,3896,PHX,LAX,AMERICA ,	2130,	2276,	1371,	1390,	T,	T,	T,	T,	T,	T,	1242,	1130
AA ,2489,DFW,LAX ,	2130,	2168,	1317,	1393,	T,	T,	T,	T,	T,	T,	1014,	1130
QF ,3055,HNL,LAX,AMERICAN,	2169,	2276,	965,	1394,	T,	T,	T,	T,	T,	T,	2088,	1130
AA ,284 ,HNL,LAX ,	2130,	2168,	965,	1397,	T,	T,	T,	T,	T,	T,	2088,	1130
QF ,3055,HNL,LAX,AMERICAN,	2130,	2168,	965,	1397,	T,	T,	T,	T,	T,	T,	2088,	1130
AA ,1891,ORD,LAX ,	2130,	2168,	1259,	1399,	T,	T,	T,	T,	F,	T,	1230,	1130
AA ,8308,MEX,LAX,MEXICANA,	2130,	2130,	1275,	1400,	F,	F,	F,	F,	F,	T,	1748,	1130
AA ,193 ,JFK,LAX ,	2130,	2168,	1260,	1432,	T,	T,	T,	T,	F,	T,	1127,	1130
QF ,3102,JFK,LAX,AMERICAN,	2130,	2168,	1260,	1432,	T,	T,	T,	T,	F,	T,	1127,	1130
UA ,9549,LAX,AKL,AIR NEW ,	2130,	2283,	1185,	330,	T,	T,	T,	T,	T,	T,	1130,	1888
UA ,9549,LAX,AKL,AIR NEW ,	1926,	1987,	1290,	315,	T,	T,	T,	T,	T,	T,	1130,	1888
UA ,9549,LAX,AKL,AIR NEW ,	1988,	2099,	1290,	315,	T,	T,	T,	T,	T,	T,	1130,	1888
UA ,9549,LAX,AKL,AIR NEW ,	2100,	2129,	1290,	375,	T,	T,	T,	T,	T,	T,	1130,	1888
UA ,9545,LAX,AKL,AIR NEW ,	1926,	1987,	1350,	375,	F,	F,	F,	T,	F,	F,	1130,	1888
UA ,9545,LAX,AKL,AIR NEW ,	1994,	2099,	1350,	375,	F,	F,	T,	F,	F,	F,	1130,	1888
UA ,9545,LAX,AKL,AIR NEW ,	2106,	2127,	1350,	435,	F,	F,	F,	T,	F,	F,	1130,	1888
UA ,9545,LAX,AKL,AIR NEW ,	2130,	2283,	1305,	450,	T,	T,	T,	T,	T,	T,	1130,	1888
UA ,9545,LAX,AKL,AIR NEW ,	1926,	1982,	1410,	435,	T,	T,	F,	T,	T,	T,	1130,	1888
UA ,9545,LAX,AKL,AIR NEW ,	1984,	1986,	1410,	435,	T,	T,	T,	F,	F,	F,	1130,	1888
UA ,9545,LAX,AKL,AIR NEW ,	1988,	1997,	1410,	435,	T,	T,	T,	F,	T,	T,	1130,	1888

Reformatted Flight Information Database

Figure 14

To understand the format of the database, a description of the columns is useful. Columns 1 and 2 are the airline name and flight number. Columns 3 and 4 are the departure and arrival airports. Column 5 is the airline operating the flight. Column 6 is the operating start day of the flight in terms of the number of days since 1 January 2000. Column 7 is the scheduled operating end day of the flight in terms of the number of days since 1 January 2000. Column 8 is the departure time of the flight in terms of the number of minutes since midnight on the day of departure. Column 9 is the arrival time of the flight in terms of the number of minutes since midnight on the day of departure. Columns 10-16 are a true table defining the operating days of the flight. For instance, a “T” in column 10 means that that particular flight operates on Monday. The last two columns contain a code relating to the arrival and departure airport.

Based on the user input of date, time of day, and region of interest from the GIS interface, the program will query the database to determine the type of aircraft, their heading and orientation, based on the time since departure, and airspeed based on distance of the airport. All of the planes of interest will be displayed on the GIS screen as shown in Figure 15. Note that the aircraft locations shown in Figure 15 are for demonstration only and do not represent any particular time of day.



GIS Feedback of Airplane Location (demonstration only)
Figure 15

The system user can also specify the location of the MANPADS launch site in the GIS system. This information is passed to the program to be used to compute the location vectors and transformation vectors. The user will have the option of choosing any of the aircraft displayed on the screen; the aircraft closest to the MANPADS launch site, or a region of aircraft collection. The program will determine the projected area, and hence the probability of hit.

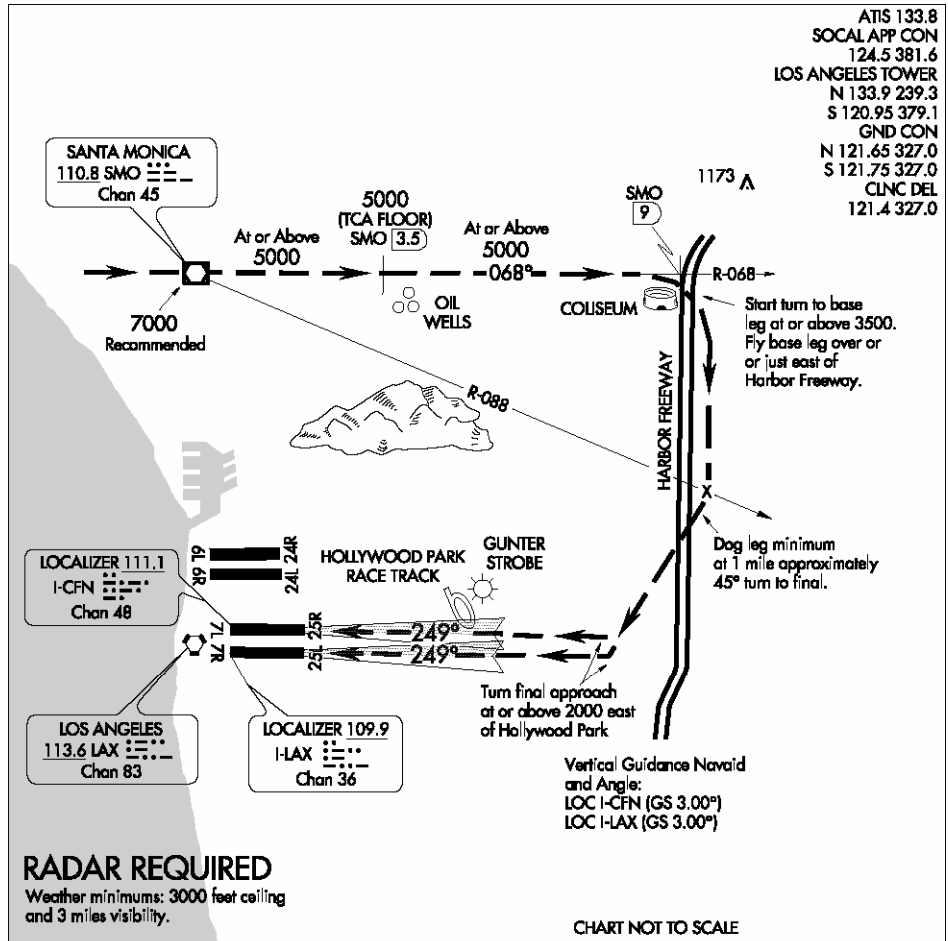
Once the program identifies the subset of aircraft in the vicinity of the airport, the program assigns one the pre-programmed arrival or departure procedures to it. These procedures are based on the Federal Aviation Administration (FAA) IFR and Visual charts. Figures 16 and 17 show two typical LAX approach charts. Figure 16 is the visual approach into LAX from the west. Figure 17 is the instrument landing system (ILS) landing using runway 24L.

Amcht 4 02332

AL-237 (FAA)

HARBOR VISUAL RWY 25L/R

LOS ANGELES INTL (LAX)
LOS ANGELES, CALIFORNIA



HARBOR VISUAL APPROACH

When visual approaches to Runways 25L/R are in progress, clearances to aircraft from the north and northwest will be given utilizing the following phraseology:

"(IDENT) CLEARED FOR HARBOR VISUAL RUNWAY 25 LEFT/RIGHT APPROACH."

A descent profile of approximately 3° starting at 7000 over SMO VOR/DME may be made with reference to the minimum altitudes above.

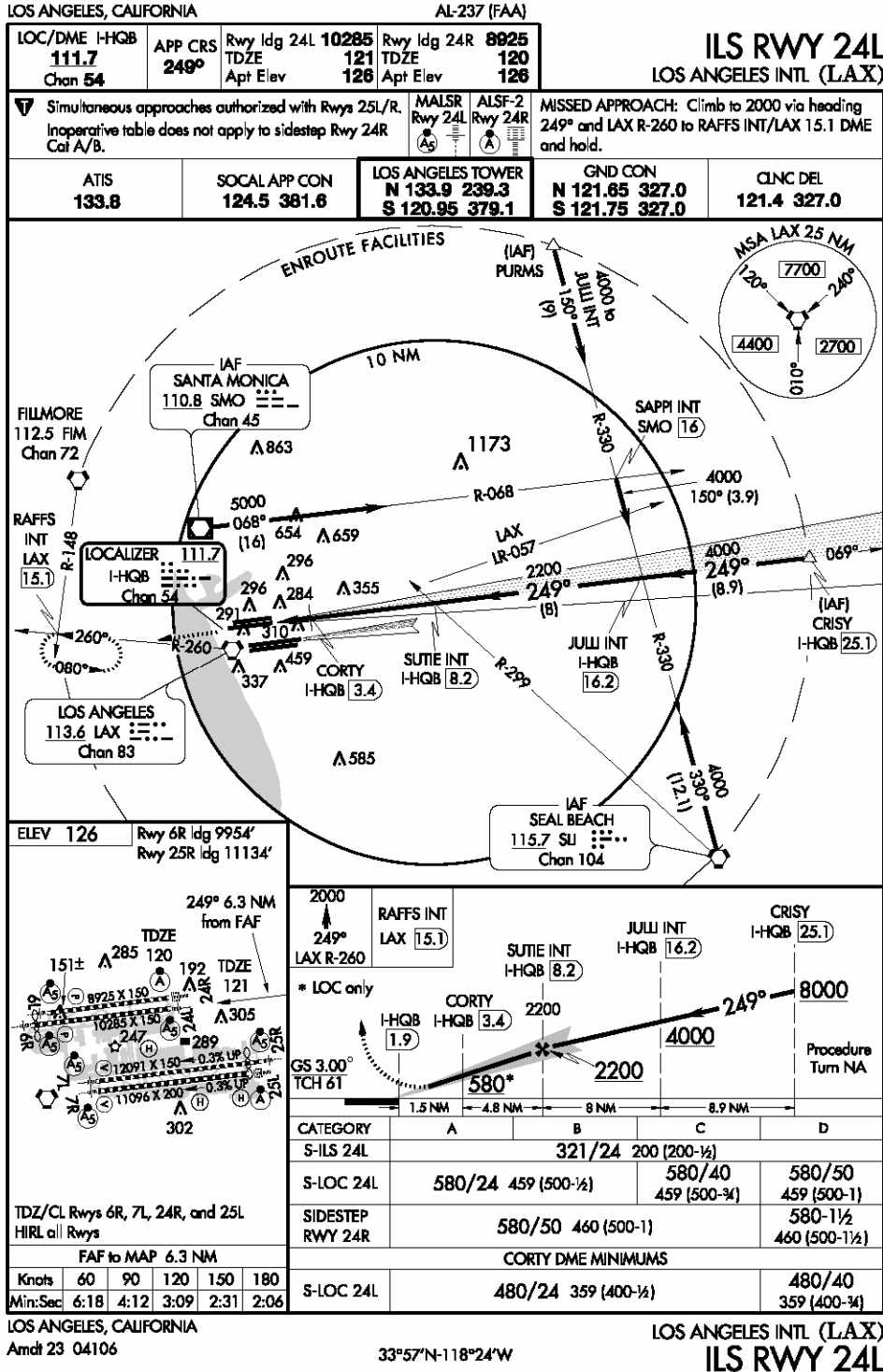
HARBOR VISUAL RWY 25L/R

LOS ANGELES, CALIFORNIA
LOS ANGELES INTL (LAX)

Amcht 4 02332

33°57'N-118°24'W

Visual Approach Into LAX from the West
Figure 16



ILS Approach Into LAX Using Runway 24L
Figure 17

Five approach procedures have been included in the program: the visual from the west, and four ILS approaches, each from one the four quadrants, that is, 45-135 degrees, 135-225 degrees, 225-315 degrees, and 315-45 degrees where 0 degrees is north.

Furthermore, for simplicity, each approach is idealized as a three-leg procedure, a straight line representing the flight path towards LA, a circular arc connecting the approach flight path to the final approach, and finally a straight line for the final approach. The end of the final leg is fixed (that is the airport), however, the other three points are treated as a constant plus a Gaussian random variable, so that no two aircraft will have exactly the same flight path.

Once an aircraft is identified as being in the vicinity of interest, it is assigned a flight path depending on the location of the departure airport and arrival airport. A unique path is then created for the aircraft approach, based on the random variables for point 1, 2, and 3, of the idealized approach. Working backward from the published arrival time, the program estimates where on the flight path the aircraft is. The preferred altitude of the aircraft at each of the three points is also modeled as a constant plus a Gaussian random variable. As can be seen, the aircraft can, theoretically, be almost anywhere in the region, although it definitely has a more likely (probable) preferred location, as is the actual case.

Following are the equations of the idealized flight path as shown in equations 1-5.

$$y_1 = M_1 x_1 + B_1 \quad (1)$$

$$(x_2 - x_c)^2 + (y_2 - y_c)^2 = R^2 \quad (2)$$

$$y_3 = M_3 x_3 + B_3 \quad (3)$$

$$x_c = .5 * (x_2^2 + y_2^2 - 2y_2 B_3 - x_3^2 - y_3^2 + 2y_3 B_3) / (x_2 + y_2 M_3 - x_3 - y_3 M_3) \quad (4)$$

$$y_c = M_3 x_c + B_3 \quad (5)$$

where

x_1 is the x coordinate of the start of leg 1

y_1 is the y coordinate of the start of leg 1

x_2 is the x coordinate of the start of leg 2

y_2 is the y coordinate of the start of leg 2

x_3 is the x coordinate of the start of leg 3

y_3 is the y coordinate of the start of leg 3

x_c is the x coordinate of the center of the arc (leg 2)

y_c is the y coordinate of the center of the arc (leg 2)

M_3 is the slope of the line representing leg 3

B_3 is the y-intercept of line representing leg 3

Equations 1-3 are the equations defining the three legs of the idealized flight path.

Equations 4 and 5 are used to determine the center of the leg 2 arc. Additional logic has

been included in the program to identify the arc length and distance along the arc for determining the aircraft position.

An idealized visual approach into LAX, using the above listed procedure, is shown in Figure 18.



Idealized Visual Approach Into LAX
Figure 18

WEAPON LETHALITY MODEL

The lethality of the MANPADS weapon is modeled using a sinusoidal tapered window as shown in Equations 6-10 below:

$$P(x)=0 \quad x \leq S1 \quad (6)$$

$$P(x)=(P_0(1 - \sin(((x - s1)/(s2 - s1)) * \pi + \frac{\pi}{2}))) / 2 \quad S1 \leq x \leq S2 \quad (7)$$

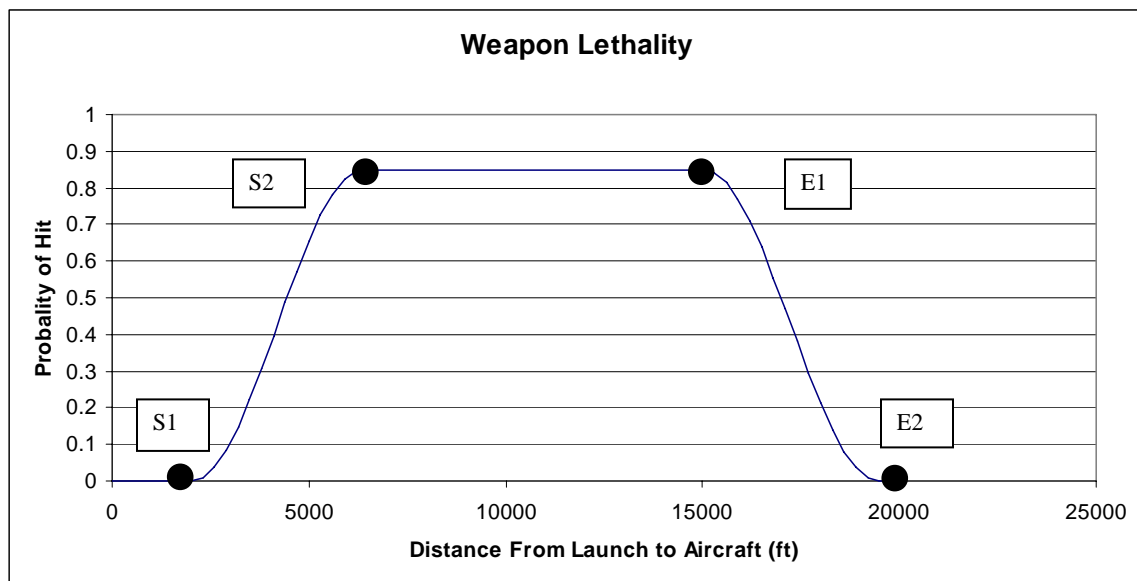
$$P(x)=P_0 \quad S2 \leq x \leq E1 \quad (8)$$

$$P(x)=P_0(1 + \sin(((x - E1)/(E2 - E1)) * \pi + \frac{\pi}{2}))) / 2 \quad E1 \leq x \leq E2 \quad (9)$$

$$P(x)=0 \quad x \geq E2 \quad (10)$$

For the example presented in the report, the nominal values of P₀, S₁, S₂, E₁, and E₂ (shown in Figure 19) are taken to be 0.85, 2000., 6400., 15000., and 19500. respectively. No attempt is made to validate these values against a real MANPADS weapon. These are

used to demonstrate the methodology only. Figure 19 shows the plot of the example MANPADS hit probability function.



Example: MANPADS Hit Probability Function
Figure 19

In the computer program implementation, the value of P_0 is not taken as a constant value but rather a Gaussian random variable with a mean of 0.85 and a standard deviation of 0.1

METHODOLOGY FOR LOCATING AIRCRAFT DEBRIS SCATTER

The debris scatter calculations are based on the physics of a falling object subjected to gravity in the vertical direction, and no imposed acceleration in the two horizontal directions, subsequent to the blast caused by a MANPADS explosion. The number of particles formed by the explosion is set by the user. In the example, the number of particles was taken to be 50. The size distribution used for the particles is based on a pseudo-Gaussian distribution generated as follows:

1. The user selects the number of particles, taken to be 50 in this example
2. The user selects a mean and standard deviation. The absolute magnitude of the mean and standard deviation is not critical, only the relative magnitude of the two parameters. For this example, the mean was taken to be 1.0 and the standard deviation was taken to be 2.0. A Gaussian distribution of 50 data points is created and an absolute sum is performed on the distribution. The resulting distribution is shown in a histogram. The rationale of the high standard deviation relative to the mean is that it is believed that an aircraft will break up into a few large pieces and many smaller pieces. It will, however, result in a substantial number of negative data points in the distribution, which

is unrealistic. Taking the absolute value eliminates the negative points, yet retains much of the Gaussian properties of the distribution.

- The next step is to scale the particle data points so that the sum of the particle masses is equal to the total mass of the aircraft (which in our example is 5947 slugs). A histogram of the resulting particle distribution is shown in Figure 20. As can be seen, a few particles have a large mass. In fact, the largest 5 particles have a total mass of 6750 out of the total mass of the aircraft of 27950. The top 10% of the particles have 24% of the mass. This is considered to be realistic.

It should be noted that a log-normal distribution, or a variety of other distributions, could have been used instead of the pseudo-Gaussian distribution described above. The log-normal distribution was not used because the above procedure gave the desired results. To change the distribution type, a new module can be added very easily.

To model the air resistance acting on the falling particles, the standard equation of a blunt object moving through air was used as shown in equation 11.

$$F_D = C_D \rho AV^2 \quad (11)$$

where

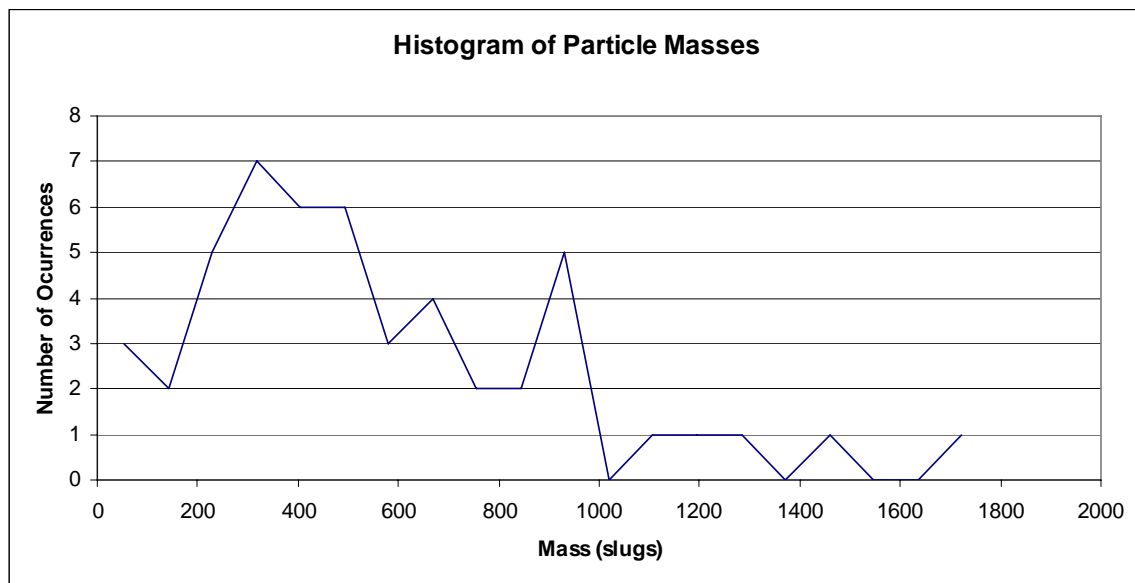
F_D = Wind drag

C_D = Coefficient of drag

ρ = Air density

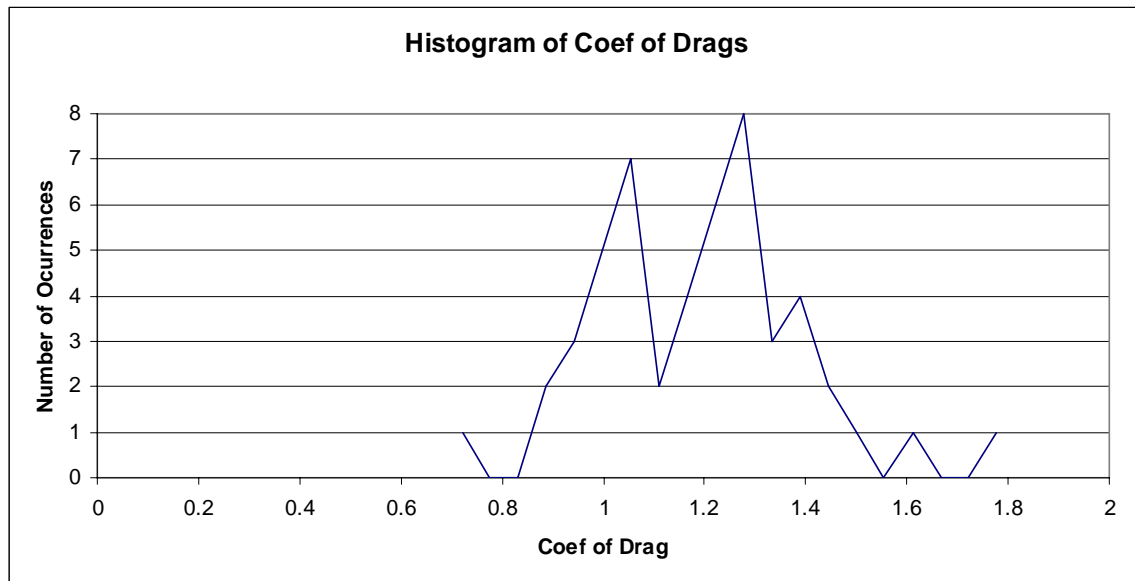
A = Exposed area

V = particle velocity



Example: Distribution of Particle Mass Size
Figure 20

The Coefficient of drag is typically about 1.2, however, the value may vary substantially, depending on the shape of the particle. For this reason, the coefficient of drag was taken as a random variable with a Gaussian distribution. For the example here, the mean value was assumed to be 1.2, with a standard distribution of 0.25. A histogram showing the actual distribution used for the coefficient of drag is shown in Figure 21. As can be seen, the values lie between 0.7 and 1.8 which is appropriate. It should be noted that there is no attempt to match the value of the coefficient of drag to the size of particles. The value of coefficient of drag is randomly assigned to each of the particles.



Example: Coefficient of Drag Distribution
Figure 21

The value of the exposed area was taken to be proportional to the particle mass. The constant of proportionality was computed by assuming that the sum of all of the volumes of the particles equal the volume of the original aircraft. Then, by assuming that each particle is a sphere, the exposed area to the air can be estimated.

The distribution of particle velocities was slightly more complicated, with the procedure used as follows:

1. The magnitude of the particle velocity change due to the MANPADS explosion is taken to be a Gaussian distribution random variable with a mean V_{mean} and standard deviation S . The value of V_{mean} is estimated by approximating the potential energy stored in two near empty tanks of jet full of fuel vapor. This potential energy is converted into kinetic energy as the plane explodes. The mean velocity calculation considers the entire aircraft mass to have the same imposed velocity. The standard deviation was taken to be 25% of the mean. This methodology used to estimate the mean and standard deviation is not rigorous, and the resulting estimates may have a large error associated with them. If the user wishes to include a more precise

estimate of the particle velocity, a new module may be easily added. Figure 22 shows the distribution of the velocity magnitudes for the 50 particles.

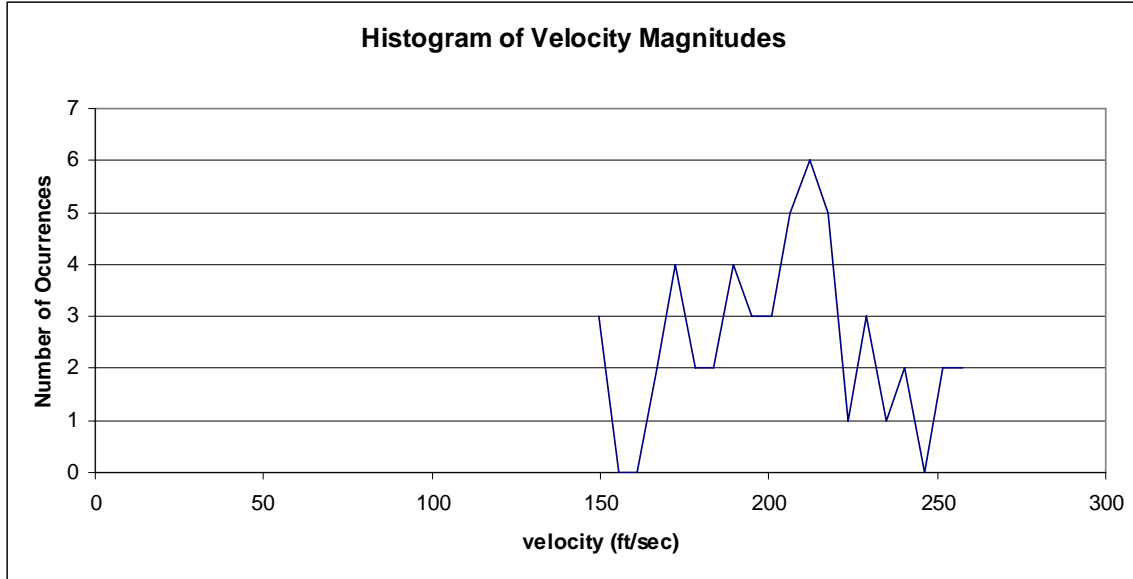
2. After the velocity magnitudes are computed for the particles, they are randomly assigned to the particles. Again, there is no attempt to correlate the particle velocity to the size of the particles.
3. For each particle, a uniformly distributed random number between -1.0 and 1.0 for each of the three directions are generated. These three random variables distribute the velocity magnitude in each of the three directions. Finally, the resulting velocity components are scaled such that the square root of the sum of the squares is equal to the assigned velocity magnitude for the particle. For example, suppose that the velocity magnitude of a particular particle was found to be 225 ft/sec from the Gaussian distribution. The same particle is assigned the uniformly distributed random variables -0.25 , 0.75 , and 0.5 for the X, Y, and Z directions. Using these as factors, the velocities in the three orthogonal directions are taken to be -60.13 , 180.4 , and 120.2 ft/sec in the X, Y, and Z directions respectively. Note:

$$\sqrt{60.13^2 + 180.4^2 + 120.2^2} = 225.0$$

which is the velocity magnitude assigned to the particle

The end result is a set of velocity vectors whose magnitudes follow a Gaussian distribution and the directions follow a uniform distribution. Histogram plots of the X, Y, and Z directions are shown in Figure 23 for the 50 particle example. Once the velocity vector is established for each of the particles, then analysis of the particles motion is ready to be performed. It should be emphasized that the velocity vectors discussed are only the initial velocity of the particles after the initial explosion and they do not include the forward velocity of the aircraft prior to the explosion.

To determine the trajectory of each of the particles, three finite difference analyses are performed on each particle, one in each of the three orthogonal directions. The first analysis is performed in the Z direction and it includes the acceleration due to gravity. The initial conditions for each of the particle analyses are the aircraft height at the time of the explosion, and initial velocity vector as described previously. The aircraft's vertical speed is considered negligible and is not included. The analysis is completed when the particle reaches the ground elevation. Next, the finite difference analysis is performed in the two horizontal directions. The duration of the horizontal direction analyses is set by the Z direction analysis, that is, the time it takes for the particle to reach the ground. In these analyses, the forward velocity of the aircraft is not negligible, and it is added to the previously computed velocity vector to form the velocity initial condition for the analysis.



Example: Distribution of Particle Velocity magnitudes
Figure 22

For convenience, the details of the finite difference analysis are shown below. The equation of motion for each of the particles follows Newton's second law.

$$\text{Force} = \text{mass} * \text{acceleration} \quad (12)$$

The force in the equation is the drag due to wind forces plus the force due to gravity, in the case of the vertical analysis. The mass term is the mass of the individual particles, and the acceleration is the acceleration of the individual particles subsequent to the explosion. The central finite difference expressions for the accelerations and velocity are as follows:

$$\text{Velocity} = (x_{n-3} - x_{n-1}) / 2\Delta t \quad (13)$$

$$\text{Acceleration} = (x_{n-2} - 2x_{n-1} + x_n) / \Delta t^2 \quad (14)$$

The applied force acting on each particle is given by:

$$F = -C_D \rho A V_{abs}(V) \quad \text{For the horizontal directions}$$

$$F = -C_D \rho A V_{abs}(V) - MG \quad \text{For the vertical direction}$$

Therefore, for the horizontal directions

$$x_n = [C_D \rho A (x_{n-3} - x_{n-1}) / 2M\Delta t |(x_{n-3} - x_{n-1}) / 2\Delta t|] \Delta t^2 + 2x_{n-1} - x_{n-2} \quad (15)$$

For the vertical direction

$$x_n = [C_D \rho A (x_{n-3} - x_{n-1}) / 2M\Delta t |(x_{n-3} - x_{n-1}) / 2\Delta t| + G] \Delta t^2 + 2x_{n-1} - x_{n-2} \quad (16)$$

Equations 15 and 16 are the difference equations for the particle motion after the explosion for the horizontal and vertical directions. The additional G term in the equation 16 represents the gravity loading in the vertical direction. Equations 15 and 16 are solved recursively, that is, the value of X_n is determined using the previous 3 times steps. Considering that the initial conditions, i.e., the initial velocity plays such an important role in the solution, it is critical to have good estimates for X_1 , X_2 , and X_3 . To this end, a preliminary analysis at a time step reduced by a factor of 10 is performed as shown in equations 17 and 18.

$$x_n = [C_D \rho A (x'_{n-3} - x'_{n-1}) / 2M\Delta t_s | (x'_{n-3} - x'_{n-1}) / 2\Delta t_s | \Delta t_s^2 + 2x'_{n-1} - x'_{n-2}] \Delta t_s^2 + 2x'_{n-1} - x'_{n-2} \quad (17)$$

$$x'_n = [C_D \rho A (x'_{n-3} - x'_{n-1}) / 2M\Delta t_s | (x'_{n-3} - x'_{n-1}) / 2\Delta t_s | + G] \Delta t_s^2 + 2x'_{n-1} - x'_{n-2} \quad (18)$$

$$\Delta t_s = \Delta t / 10$$

The initial conditions for equations 17 and 18 are given by:

$$x'_2 = X_0$$

$$x'_1 = [C_D \rho A V_0 \text{abs}(V_0) / M] \Delta t_s^2 - V_0 \Delta t_s x'_2 \quad (19)$$

$$x'_3 = 2V_0 \Delta t_s + x'_1$$

Equations 17 and 18 are used for 21 iterations at the reduced time step. These results of this preliminary analysis are used to set the initial conditions for the complete analysis at the larger time step. The initial conditions are shown in equation 20.

$$\Delta t_1 = \Delta t_{s1}$$

$$\Delta t_2 = \Delta t_{s11} \quad (20)$$

$$\Delta t_3 = \Delta t_{s21}$$

The finite difference analysis was applied to the 50 particle example. The resulting velocities and displacements are shown in Figure 23. The following observations are noted regarding the results shown:

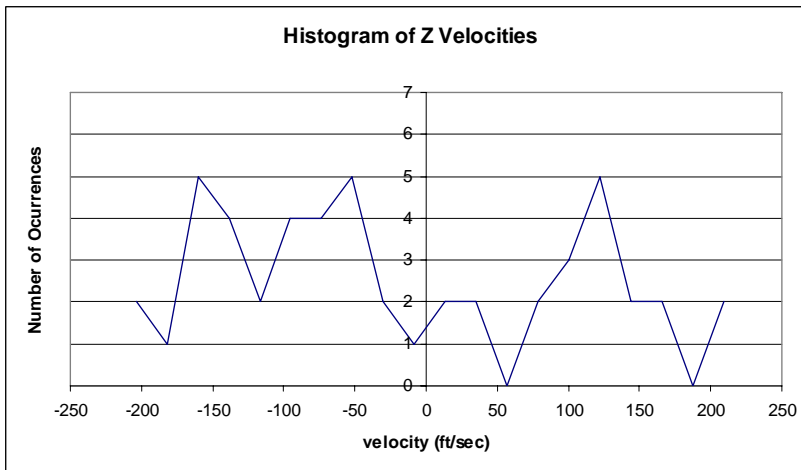
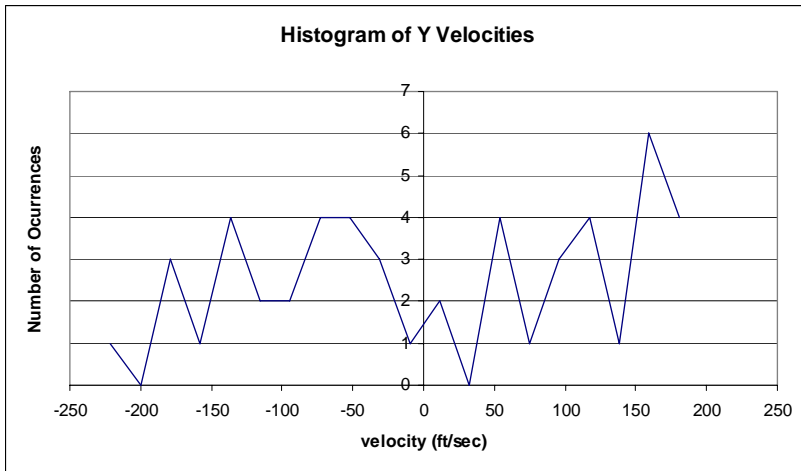
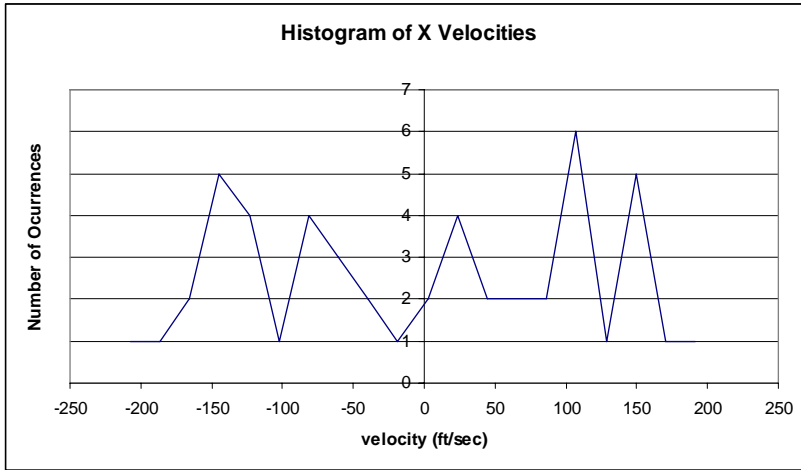
1. The initial velocities for all three directions are different. The X direction initial velocity includes the forward velocity of the aircraft, which is assumed to be traveling in the X direction only.
2. The velocity in the Z direction approaches the terminal velocity of the particle, which is when the force due to gravity equals the air drag force. The velocities in the X and Y directions approach zero, as only the wind drag force acts on the particle after the explosion.
3. The displacement in the Z direction starts at 1500 ft, which is the aircraft's altitude at the time of the missile hit. The displacement in the X and Y

directions starts at 0.0, so the results are the relative displacement of the particles from the location of impact.

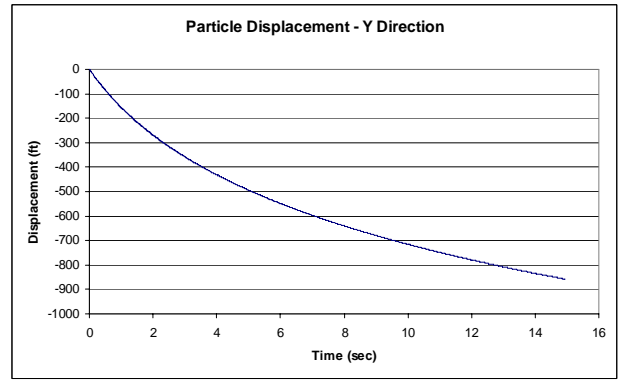
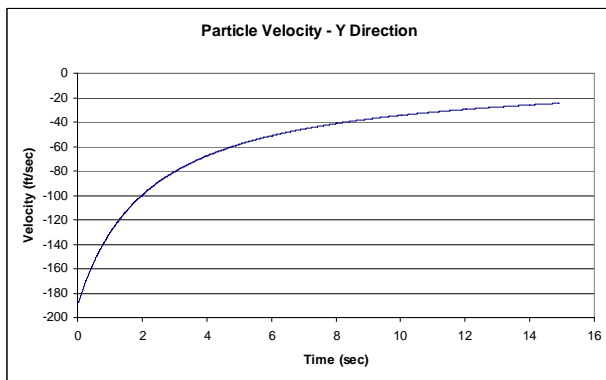
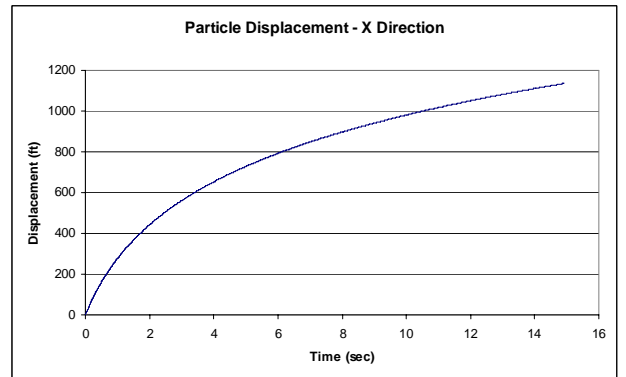
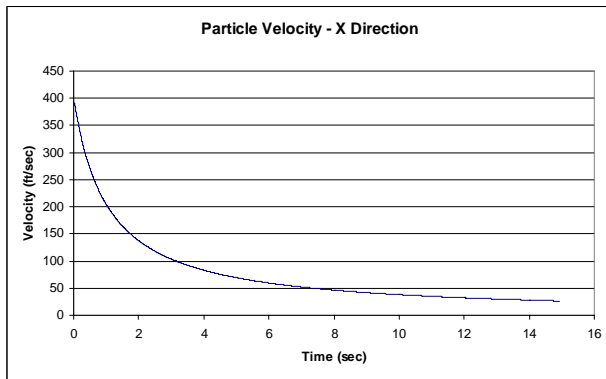
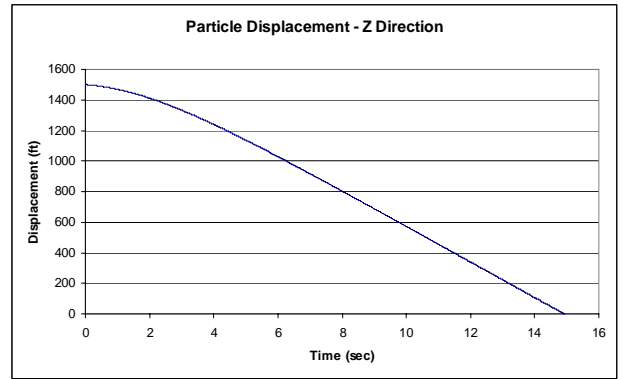
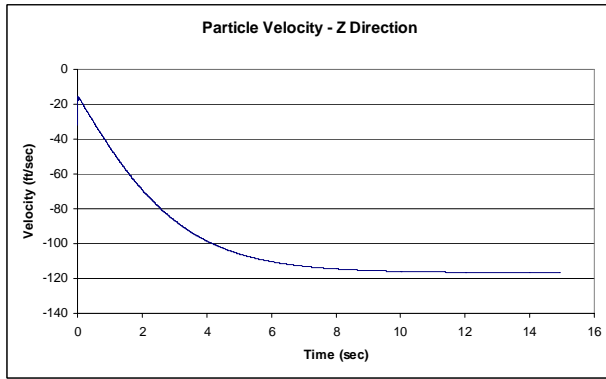
4. The analysis ends when the particle displacement in the Z direction equals zero, as that indicates that the particle has hit the ground. The analysis for the X and Y directions also end at the same time, and the final values represent the location of the particle on the ground relative to the impact location.

Figures 23 and 24 shows the results for only the first particle of the 50 particles in the study. For all 50 particles, a total of 150 finite difference solutions with a Δt of 0.01 seconds. While this seems to be a large number of calculations, the loops are tight therefore. The total solution for all 50 particles was complete in less than a second. In the released version of the computer program, only the final displacement of the particles will be stored. Figure 25 shows the results of the particle scatter in terms of the distance that the debris hits the ground relative to the impact location. The computer program also generates a table containing the GIS coordinates of the debris, giving the GIS location of the aircraft at the time of impact.

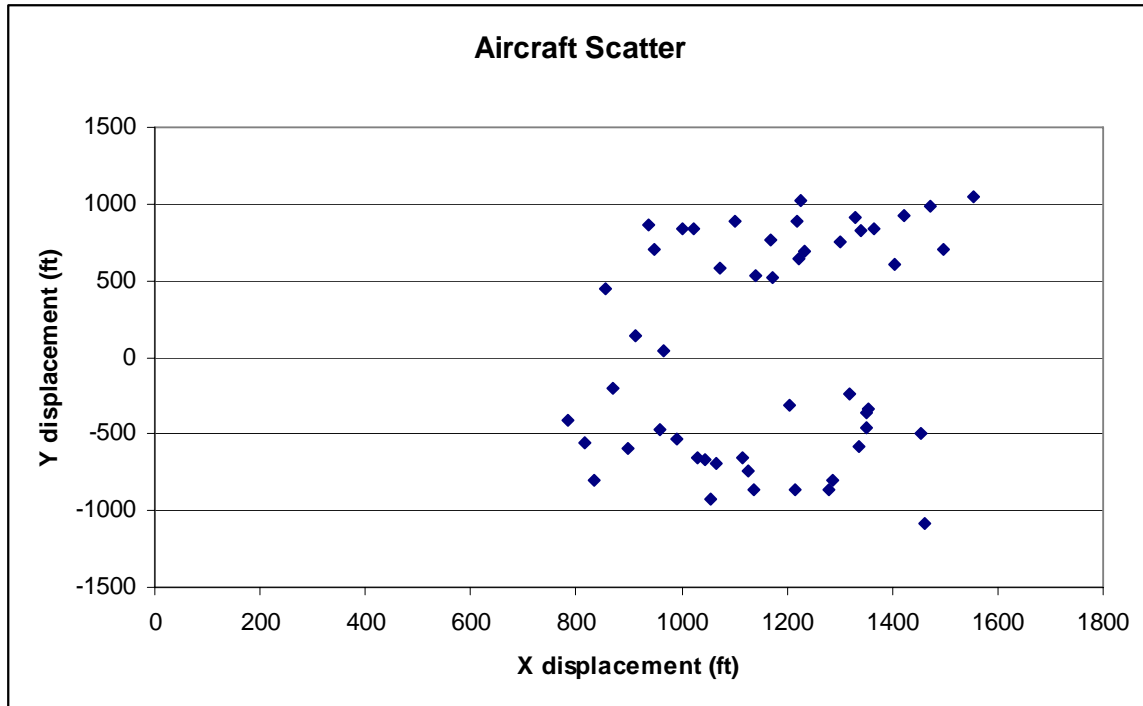
The results shown in Figure 26 provide valuable information for the researcher. The aircraft is located at coordinate 0.0 on the plot. The value on the scatter can be seen to extend about 1200 ft to each side and about 1600 ft in the direction of the aircraft. When plotted on the GIS map, the specific location of the debris scatter can be identified. By performing scatter calculations several times, one can get a good estimate as to where the critical areas are in the LA basin for planning purposes.



Example: Histogram of Initial Velocities
Figure 23



Example: Velocity and Displacement Time Histories of Particle #1
Figure 24



Example: Aircraft Debris Scatter
Figure 25

POTENTIAL RESEARCH

Expanding the General Probabilistic Methodology for Multi-Aircraft/Multi-Weapon Attacks

The computer program's main driver routine may be modified to handle the case of multiple aircraft in the region. The GIS interface could be updated to allow the user to specify region of interest to establish the collection of vulnerable aircraft to the considered.

The modification/additions to the current computer program will entail:

- by repeating the above procedure for each aircraft in the landing path, as well as the take-off path, the expected failure probabilities for the collection of vulnerable aircrafts can be obtained as $\{F_1, F_2, \dots, F_n\}$.
- assuming a single attack (weapon launch), then the worst case scenario would correspond to the largest probability among the set of n probabilities computed above:

$$F_{\max} = \max_n \{F_1, F_2, \dots, F_n\}$$

- the procedure discussed so far will yield the most likely probability of aircraft failure assuming the launch site is at one specific bloc area of size A_0 . By repeating the same analysis with many other blocks surrounding the target airport, one can construct a 3D probabilistic damage surface in which the two horizontal axes correspond to the ground surface region of interest, and the vertical axis would correspond to $F_{\max}(A_{0,x}, A_{0,y})$
- the topology of the above mentioned damage surface can be quite useful to the authorities in establishing the most vulnerable locations surrounding a given airport, at a specific time and on a specific day.
- depending on the postulated attack scenario (e.g., a single attack of multiple attacks), the analysis/simulation procedure discussed above, can be generalized to evaluate any desired scenario of multiple attacks.
- in the case of multiple attacks, if it is assumed that a single aircraft is subjected to two “shots”, then if the probability of the aircraft being destroyed by a single shot is P_{k1} , then the probability of not being destroyed is $1 - P_{k1}$. Therefore, the probability of being destroyed by the second shot, given that it survived the first shot is $P_{k2} = (1 - P_{k1})P_{k1}$. Consequently, the probability that the aircraft is destroyed in a two-shot engagement is:

$$P_{k1} + P_{k2} = P_{k1} + P_{k1}(1 - P_{k1}) = P_{k1}(1 + 1 - P_{k1}) = P_{k1}(2 - P_{k1})$$

CONCLUSIONS

In view of the numerous uncertain decision and performance variables encountered in the modeling of scenarios involved in the assessment of the consequences of MANPADS attacks on civilian aircraft, there is a need for the development of a general probabilistic methodology for multi-aircraft/multi-weapon attacks.

This report presents an initial stage of a general methodology for developing and implementing a modular software package that incorporates a variety of computational modules for quantifying and propagating the uncertainties associated with the specification of a postulated terrorist attack. Among the main random parameters considered are: the aircraft location and orientation, the aircraft flight path trajectory, the aircraft characteristics, the probability of a weapons-induced crash, and the random distribution of explosion debris, etc.

While an arbitrary scenario was used to demonstrate the implementation of all phases of the chain of events encompassing the randomness imbedded in the numerous input parameters to the computational engine, the systems-based architecture is extremely flexible, and would easily allow the user to replace specific modules with updated ones that reflect needed levels of analysis sophistication, weapons performance data, structural failure analysis, aircraft equipment vulnerability data, more accurate physics-based modeling of debris dispersal, etc.

In order to maximize the utility of the simulation package, its modules are designed to easily interface with a GIS-based package in which other related threat and consequence scenarios can be conveniently specified, and their outcomes evaluated and displayed in near real time, to assist decision makers in quickly investigating a broad range of postulated attack scenarios.

REFERENCES

Ball, R E, (2003), *The Fundamentals of Aircraft Combat Survivability Analysis and Design*, American Institute of Aeronautics and Astronautics, Inc., Reston, VA.

Bathe, Klaus-Jurgen, *Finite Element Procedures*, Prentice Hall, 1996.

Bolkcom, C., Elias, B., Feickert, A., *Homeland Security: Protecting Airlines from Terrorist Missiles*, CRS Report for Congress, November 3, 2003.

O'Sullivan, Terry, *External Terrorist Threats to Civilian Airlines: A Summary Risk Analysis of MANPADS, Other Ballistic Weapons Risks, Future Threats, and Possible Countermeasures Polices*, Draft, October 2004.

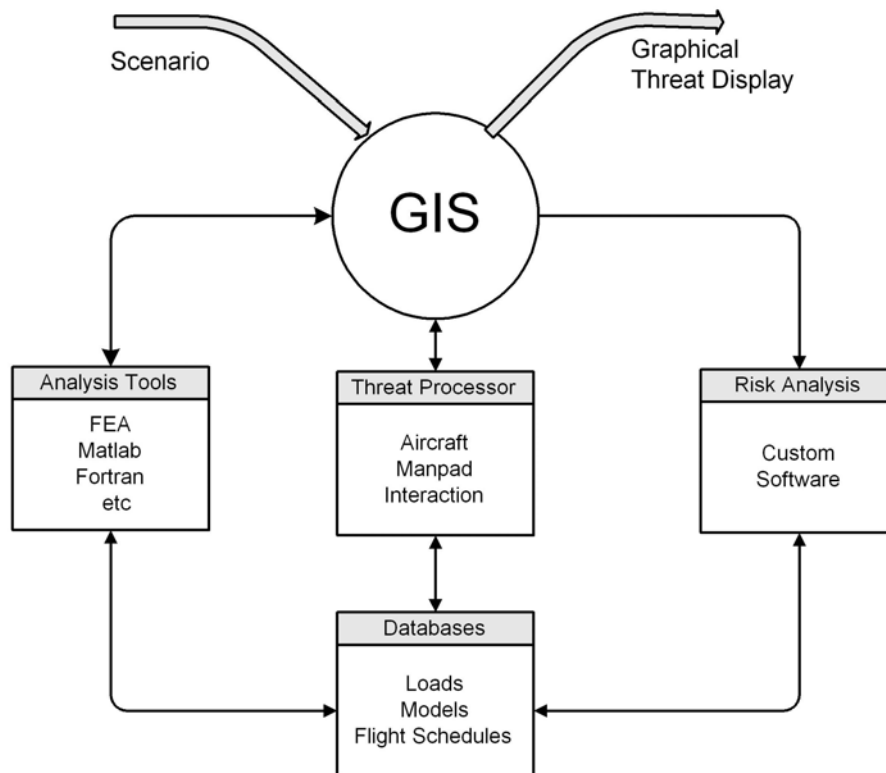
United States General Accounting Office, *Subject: The Department of Homeland Security Needs to Fully Adopt a Knowledge-Based Approach to Its Counter-MANPADS Development Program*, January 30, 2004

Wesenberg, Donald L., (2004), Private Communication, Sandia National Laboratory, 29 September 2004. dlwesen@sandia.gov.

Appendix 1 GIS INTERFACE DESIGN DOCUMENT

The general program flow is shown in Figure 1. The GIS program should run the FORTRAN executables without user interaction. All database files and intermediate interface files should be located in a predetermined folder location.

The purpose of this document is to define the data exchange between the GIS interface and the FORTRAN executables.



GIS Flowchart
Figure 1

There are to be three parts to interface to the GIS system. Each part is individual with all of processing contained within one Fortran module. The document describes the interface to each of three Fortran modules

PART ONE

The first part creates the map of the Los Angeles basis with markers to indicate the locations of the aircraft at any particular time and date. The users initiates this feature through the GIS system. The interface passes information to the GetAircraft module in

the form of an ASCII file. The file generated by the GIS program should contain 6 lines as follows:

```
1      Indicates that the file is new
HH:MMxm
XXX
YY
x1.xxxxx, y1.yyyyy
x2.xxxxx, y2.yyyyy
```

where: HH:MMxm Time of day
 HH - Hour 1-12
 MM - Minute 00-59
 xm - Am or PM

 XXX Month JAN, FEB, up to DEC
 YY Date 1-31
 ZZZZ- Year, 2005 etc

 x1.xxxxx Far south latitude of the map
 y1.yyyyy Far west longitude of the map
 x2.xxxxx Far north latitude of the map
 y2.yyyyy Far east longitude of the map

Notes: Latitudes may be positive or negative
 File name is to be GISOUT1.TXT located in the directory C:\HLSFILES
 Example files are attached

After the file GISOUT1.TXT is created, the GIS program executes the module c:\HLSCODE\getaircraft.exe. The GetAircraft module creates an ASCII file named GISIN1 located in the c:\HLSCODE of the form:

```
1      Indicates that the file is new
Day   Monday, Tuesday, etc
N1    Number of minutes since midnight, not used at this time
N2    Number of days since Jan 1, 2000, not used at this time
N3    Number of data points to follow
data  XXX YYY AA FFF
      x1.xxxx  y1.yyyyy  z1.zzzzz
      x2.xxxx  y2.yyyyy  z2.zzzzz
      x3.xxxx  y3.yyyyy  z3.zzzzz
data ...
```

where: XXX - Arriving airport designation
 YYY - Departing airport designation
 AA - Airline

FFF	Flight Number
x1.xxxx	Latitude of arriving airport
y1.yyyyy	Longitude of arriving airport
z1.zzzzz	Elevation of arriving airport
x2.xxxx	Latitude of originating airport
y2.yyyyy	Longitude of originating airport
z2.zzzzz	Elevation of originating airport
x3.xxxxx	Latitude of the aircraft
y3.yyyyy	Longitude of the aircraft
z3.zzzzz	Elevation of the aircraft

After the file GISIN1.TXT is created, the GIS program should read the file and plot the results on the map. A marker should be used to indicate the location of the Aircraft and any airports in the map area. A solid line should be used to connect the departing airport to the aircraft and a dashed line should be used to connect the aircraft to the arriving airport.

PART TWO

The second part is used to displace the location and trajectory of the missile launch. For this interface, the user selects the location of the missile launcher using the graphical interface and optionally an aircraft on the screen. These locations are written to an ASCII file names GISOUT2.TXT located in the c:\HLSCODE directory

1 Indicates that the file is new
x1.xxxxx y1.yyyyy z1.zzzzz
x2.xxxxx y2.yyyyy z2.zzzzz

where x1.xxxx Latitude of the missile launch location
y1.yyyyy Longitude of the missile launch location
z1.zzzzz Elevation of the missile launch location
(0.0 indicates that the elevation of the missile launch
 elevation is unknown)
x2.xxxx Latitude of aircraft of interest
y2.yyyyy Longitude of aircraft of interest
z2.zzzzz Elevation of aircraft of interest
(0.0 indicates that the elevation of the aircraft
 elevation is unknown)

(x2.xxxxx y2.yyyyy z2.zzzzz) -> (0. 0. 0.)
Indicates that no aircraft was specified.

After the file GISOUT2.TXT is created, the GIS program executes the module c:\HLSCODE\getprob.exe. The GetProb module creates an ASCII file named GISIN2 located in the c:\HLSCODE of the form:

```
1      Indicates that the file is new
xxx
x.xxxxx   y1.yyyyy   z1.zzzzz
x2.xxxxx   y2.yyyyy   z2.zzzzz
```

where xxx probability of hit
 x1.xxxx Latitude of the missile launch location
 y1.yyyyy Longitude of the missile launch location
 z1.zzzzz Elevation of the missile launch location
 x2.xxxx Latitude of the missile hit location
 y2.yyyyy Longitude of the missile hit location
 z2.zzzzz Elevation of the missile hit location

The GIS program should read the GISIN2.TXT file and display the missile hit location as a marker and launch path as line between the missile launch site and the hit location.

PART THREE

This part is similar to part two except that the Fortran GetScatter module returns the scatter location assuming that hit occurs. The user selects an aircraft on the screen and a missile launch location and requests a scatter pattern be generated. The GIS program creates a ASCII file named GISOUT3.TXT located in the c:\HLSCODE directory that contains the following:

```
1      Indicates that the file is new
x1.xxxxx   y1.yyyyy   z1.zzzzz
x2.xxxxx   y2.yyyyy   z2.zzzzz
```

where x1.xxxx Latitude of the missile launch location
 y1.yyyyy Longitude of the missile launch location
 z1.zzzzz Elevation of the missile launch location
 (1.0 indicates that the elevation of the missile launch
 elevation is unknown)
 x2.xxxx Latitude of aircraft of interest
 y2.yyyyy Longitude of aircraft of interest
 z2.zzzzz Elevation of aircraft of interest
 (1.0 indicates that the elevation of the aircraft
 elevation is unknown)

After the file GISOUT3.TXT is created, the GIS program executes the module c:\HLSCODE\getscatter.exe. The GetScatter module creates an ASCII file named GISIN3.TXT located in the c:\HLSCODE of the form:

1 Indicates that the file is new

num

x.xxxxx y1.yyyyy z1.zzzzz

x2.xxxxx y2.yyyyy z2.zzzzz

d1.xxxxx e1.yyyyy f1.zzzzz

d2.xxxxx e2.yyyyy f2.zzzzz

d3.xxxxx e3.yyyyy f3.zzzzz

.

.

.

dn.xxxxx en.yyyyy fn.zzzzz

where xxx number of scatter parts
 x1.xxxx Latitude of the missile launch location
 y1.yyyyy Longitude of the missile launch location
 z1.zzzzz Elevation of the missile launch location
 x2.xxxx Latitude of the missile hit location
 y2.yyyyy Longitude of the missile hit location
 z2.zzzzz Elevation of the missile hit location
 d1.xxxx Latitude of scatter location 1
 e1.yyyyy Longitude of scatter location 1
 f1.zzzzz Elevation of scatter location 1
 d2.xxxx Latitude of scatter location 2
 e2.yyyyy Longitude of scatter location 2
 f2.zzzzz Elevation of scatter location 2
 .
 .
 .
 dn.xxxx Latitude of scatter location n
 en.yyyyy Longitude of scatter location n
 fn.zzzzz Elevation of scatter location n

After the module GetScatter completes, the GIS read the GISIN3.TXT file and displays the debris scatter. If possible, the GIS program should draw an envelope around the scatter locations.